Isolation of a pentadienyl-type radical featuring a central secondary carbon

Ying Kai Loh,*a Levan Gojiashvili,a Mohand Melaimi,a Milan Gembicky,a Dominik Munz,b Guy Bertrand*a

SUMMARY: Stable tertiary (3°) R₃C· carbon radicals have been known since Gomberg's pioneering discovery of the triphenylmethyl radical more than a century ago. In stark contrast, secondary (2°) R₂CH· and primary (1°) RCH₂· carbon radicals are hitherto elusive species only observed spectroscopically Herein, we describe the isolation of a crystalline pentadienyl-type radical, featuring a central secondary carbon center, prepared by single-electron reduction of a bis(imino)carbene conjugate acid. The key to its stability is the presence of two N-heterocyclic imine (NHI) substituents, which impart both steric protection and electronic stabilization. DFT calculations confirm that the central secondary carbon is the principal spin carrier. Accordingly, EPR spectroscopy reveals that the hydrogen atom attached to the central carbon exhibits an exceptionally large hyperfine coupling constant (> 10 G) – the largest recorded for an isolated organic radical. In the presence of an H· donor, hydrogen atom abstraction occurs exclusively at the central carbon to form a methylene unit. Furthermore, this radical can participate in a radical-radical cross-coupling reaction with TEMPO [(2,2,6,6-tetramethylpiperidin-1-yl)oxyl] – the first example between two stable organic radicals.

^a UCSD–CNRS Joint Research Laboratory (IRL 3555), Department of Chemistry and Biochemistry, University of California, San Diego, La Jolla, California, USA.

^b Coordination Chemistry, Saarland University, Campus C4.1, 66123 Saarbrücken, Germany.

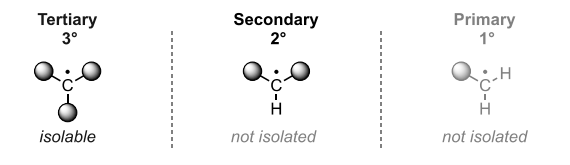
^{*} e-mail: yloh@ucsd.edu; gbertrand@ucsd.edu

Carbon radicals occupy a central role in organic chemistry. They can be categorized into three classes based on the degree of substitution - primary (1°) RCH₂•, secondary (2°) R₂CH· and tertiary (3°) R₃C· (Fig. 1A). The triphenylmethyl radical Ph₃C·, discovered by Gomberg in 1900, is the textbook example of a stable tertiary carbon radical¹. Having three phenyl substituents surrounding the radical center, the unpaired electron benefits from maximum steric protection and electronic delocalization. This design principle is now widely used to furnish carbon radicals within large networks of fused aromatic rings, which have found widespread applications in the design of organic open-shell materials². In stark contrast, secondary and primary radicals have only been observed spectroscopically, thus far eluding isolation³. It is well-established that the degree of substitution has a profound influence on the stability of carbon radicals. For instance, the C-C bond strength for the dimers of 1° (363 kJ mol⁻¹) and 2° (354 kJ mol⁻¹) radicals are significantly higher than for 3° (323 kJ mol⁻¹) radicals⁴. Although never isolated, secondary and primary carbon radicals have been identified as kev intermediates in enzymatic catalysis⁵. For instance, anaerobic microbial metabolism involves a glycyl 2º radical which is formed via hydrogen atom abstraction by 5'deoxyadenosyl 1° radical (Fig. 1B)⁶.

Recently, stable singlet carbenes such as N-heterocyclic carbenes (NHCs)^{7,8,9} and cyclic (alkyl)(amino)carbenes (CAACs)^{10,11,12} have emerged as powerful platforms to access discrete carbon radicals^{13,14,15}. In 2004, Clyburne *et al.*¹⁶ attempted to prepare a secondary carbon radical via the single-electron reduction of an NHC conjugate acid (Fig. 1C). However, the desired radical could not be observed due to the spontaneous loss of H₂ yielding the NHC. More recently, Mandal *et al.*¹⁷ reported the single-electron reduction of an abnormal NHC^{18,19} conjugate acid. While this paramagnetic species could be isolated, the unpaired electron is mainly localized on the C2 atom and its phenyl substituent, with no spin density residing on the secondary carbon center.

We recently reported the preparation of an acyclic bis(imino)carbene, ^{20,21} bearing CAAC-based N-heterocyclic imine (NHI)^{22,23,24} substituents. Herein, we report that the single-electron reduction of the bis(imino)carbene conjugate acid leads to a pentadienyl-type radical, featuring a secondary central carbon (Fig. 1D). The reactivity of this species is discussed, including a radical-radical cross-coupling reaction with TEMPO [(2,2,6,6-tetramethylpiperidin-1-yl)oxyl] – the first example between two stable organic radicals.

A. Classes of carbon radicals



B. 2° and 1° radicals in biology

C. Previous attempts at 2° radicals

D. This work

$$\begin{array}{c|c} \text{Dipp} & \text{Dipp} \\ N & N & N \\ \hline N & N & N \\ N & N \\ \hline N & N & N \\ N & N & N \\ \hline N & N & N \\ N & N & N \\ \hline N & N & N \\ N & N \\ \hline N & N & N \\ N & N \\ \hline N & N & N \\ N & N \\ \hline N & N & N \\ N & N \\ \hline N & N & N \\ N & N \\ \hline N & N & N \\ N$$

Fig. 1 | **Carbon radicals. A**, Classes of carbon radicals. **B**, 2° and 1° radicals in biology. **C**, Previous attempted synthesis of 2° carbon radicals. **D**, Present work on the synthesis and isolation of a crystalline pentadienyl-type radical, featuring a secondary central carbon.

Results and Discussion

Synthesis and characterization of the diazapentadienyl radical 1H: The cyclic voltammogram of the bis(imino)carbene conjugate acid $1H^+$ revealed a reversible single-electron redox event at -1.77 V, alluding to the generation of a long-lived radical (Fig. 2). Notably, this redox potential is significantly more negative than those observed for other isolated CAAC-stabilized carbon monoradicals (-0.30 to -1.26 V) 25,26,27,28,29 and is within the range of organic superelectron donors 30,31 .

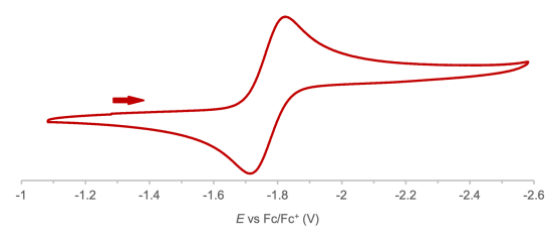


Fig. 2 | **Electrochemical studies.** Cyclic voltammogram of **1H**⁺ ([ⁿBu₄N][PF₆] 0.1 M in THF at 100 mV s⁻¹).

Motivated by this observation, we attempted the synthesis of radical 1H· on a preparative scale. Reduction of 1H⁺ with magnesium in THF afforded an NMR-silent deep purple solution (Fig. 3A). Single crystals were obtained by slow evaporation of a concentrated benzene solution, and X-ray diffraction analysis unambiguously confirmed the identity of the paramagnetic species as radical 1H, featuring a disubstituted carbon center (Fig. 3B). The central carbon adopts a trigonal planar geometry where the two NHI substituents subtend an angle of 114.5(2)° about C1. Interestingly, the central C1-N1 and C1-N2 distances [mean: 1.360(2) Å] are considerably larger than the terminal C2-N1 and C3-N2 distances [mean: 1.285(2) Å]. This stands in marked contrast to the similar central [mean: 1.311(2) Å] and terminal [mean: 1.318(2) Å] C-N bond distances displayed by 1H⁺ (for SC-XRD Supplementary Table 2). This implies that unlike 1H⁺, which has its positive charge fully delocalized across the CNCNC framework, the unpaired electron of 1H· is primarily localized on the central carbon C1. Nevertheless, the CAAC units of 1H· are essentially coplanar with the central CH motif, hinting at some degree of delocalization of the unpaired electron onto the peripheral CAAC units.

In the solid state and under argon atmosphere, radical **1H**· is stable for several weeks. However, according to EPR monitoring, its half-life time is 18 hours, when crystals are exposed to air (Supplementary Fig. 3). In solution, at room temperature, under inert atmosphere, no decomposition was observed after several weeks. In contrast, exposure of the solution to air instantaneously resulted in the disappearance of the EPR signal. No dimerization of radical **1H**· was observed even under heating at 80 °C. This is in agreement with calculations (r²SCAN-3c) that revealed that the Gibbs Free Energy for radical dimerization is prohibitively high (323 kJ mol⁻¹) (Supplementary Fig. 27).

DFT calculations performed at the r2SCAN-3c level of theory accurately reproduced the structural parameters of radical 1H· (Supplementary Table 7). The SOMO of 1H· is delocalized across the CNCNC framework, albeit with a large contribution from central C1 (Fig. 4B). Importantly, the terminal C2–N1 and C3–N2 bonds possess π bonding character, whereas the central C1–N1 and C1–N2 linkages are anti-bonding in nature, accounting for the bond distances observed in the crystal structure.

A. Synthesis of radical 1H•

B. Solid-state structure of 1H.

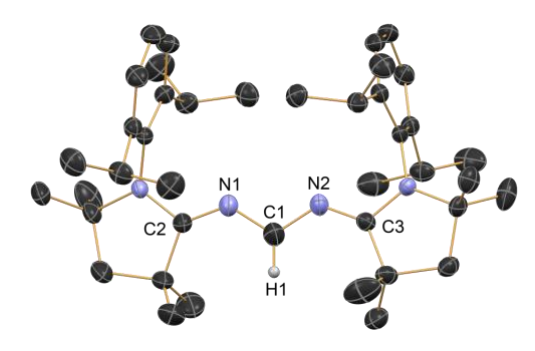
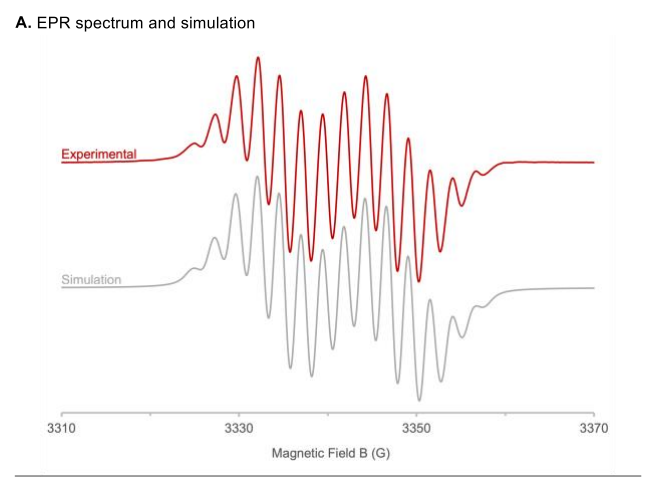


Fig. 3 | Synthesis and characterization of radical 1H·. A, Reduction of 1H⁺ with magnesium powder in THF at room temperature to afford 1H·. B, Solid-state structure of 1H· at 100 K. H atoms omitted for clarity, except H1. Thermal ellipsoids set at 50% probability.

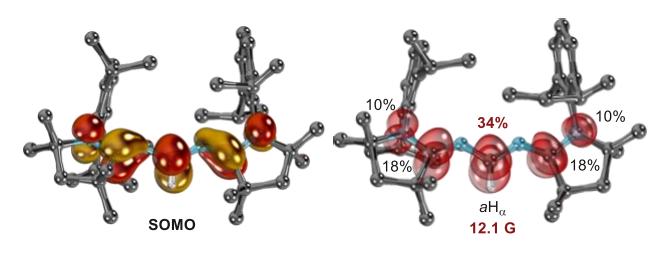
EPR analysis of 1H· confirmed the presence of an unpaired electron with a signal centered at g = 1.997 (Fig. 4A). Most strikingly, H1 which is directly attached to the 2° carbon exhibits an exceptionally large hyperfine coupling constant $aH_{\alpha} = 12.1$ G (calculated: 12.6 G; Supplementary Table 7) (Fig. 4B). This is to our knowledge the largest hyperfine coupling constant to a hydrogen atom observed for an isolated organic paramagnetic species, reflecting the pronounced spin density on C1. On the other hand, the four nitrogen atoms exhibit hyperfine coupling constants of aN =2.4 G. Löwdin atomic spin-density analysis confirmed that the 2° carbon C1 is the principal spin carrier of 1H· with a spin density of 34%. This value is slightly lower than those calculated for the diphenylmethyl Ph₂CH· (53%), triphenylmethyl Ph₃C· (49%), pentadienyl (H₂C=CH)₂CH· (43%) and obviously 2-propyl Me₂CH· (88%) radicals (Fig. 4C, Supplementary Fig. 26). 32,33,34 The remaining spin density of 1H· is delocalized across the CAAC carbon C2/C3 (18%) and nitrogen atoms (10%).

For secondary carbon radicals, the value of aH_{α} correlates with the spin density residing on the 2° carbon³⁵. Unsurprisingly, the aH_{α} in 1H• is much smaller than that of the parent 2° radical Me₂CH• which features a purely localized unpaired electron (Fig. 4C). However, it is within the range of that of diphenylmethyl radical Ph₂CH• which benefits from spin delocalization onto two phenyl rings. In fact, the aH_{α} in 1H• is very similar to that of the pentadienyl radical $(H_2C=CH)_2CH$ •³⁶, highlighting their isoelectronic relationship. Furthermore, it has been shown that there is a linear correlation between aH_{α} and resonance stabilization energies (RSEs) – a thermodynamic quantification for radical stability³⁵. Accordingly, calculations at the DLPNO-CCSD(T)/def2-TZVPP//r²SCAN-3c level of theory revealed that the RSE for 1H• is -112 kJ mol⁻¹, suggesting that 1H•

has a thermodynamic stability between Ph_2CH and $(H_2C=CH)_2CH$ (Fig. $4C)^{37}$.



B. SOMO (left), Löwdin atom spin-density and EPR aH_{α} (right)



C. Comparison of aH $\!\alpha,$ RSE and Löwdin atom spin-density of 1H $\!\bullet$ with other radicals

	Me Me	Ph C H	Ph Ph	CAAC [®] CAAC	C H
aH_{a}	21.9 G	14.7 G	_	12.1 G	11.6 G
RSE (kJ mol ⁻¹) -24	-90	-	-112	-118
Atom spir density	n _{88%}	53%	49%	34%	43%

Fig. 4 | EPR and DFT studies of radical 1H·. A, Experimental EPR spectrum (red) and simulation (grey). B, SOMO (left), Löwdin atomic spin-density and EPR aH_{α} (right). C, Comparison of aH_{α} (experimental), RSE (calculated) and Löwdin atomic spin-density values of 1H· with other transient carbon radicals.

Radical-radical cross-coupling reaction of radical 1H-with TEMPO. Radical-radical cross-couplings have recently gained attention as a complementary pathway to traditional two-electron processes^{38,39}. In stark contrast to the well-studied classical nucleophile-electrophile cross-couplings, the direct coupling reaction of two stable organic radicals is hitherto unknown. When 1 equivalent of TEMPO [(2,2,6,6-tetramethylpiperidin-1-yl)oxyl] was added at room temperature to a hexanes solution of 1H·, we observed the formation 1H-TEMPO, which was isolated as a white solid in 45% yield (Fig. 5A). X-ray diffraction analysis unambiguously confirmed the tetrahedral geometry of C1 with a newly formed C1–O1 bond (Fig. 5B). This bond is slightly elongated (1.459(1) Å), probably due to the crowded

nature of TEMPO and electron-donating properties of the NHI substituents. Note that the potential for the couple TEMPO/TEMPO⁻ ($E_{1/2} = -2.38$ vs Fc/Fc⁺)^{40,41} is more negative than that of **1H**⁺/**1H**· (-1.77 vs Fc/Fc⁺), which renders a single-electron transfer/recombination mechanism unlikely.

A. Reactivity of 1H. Dipp Dipp TEMPO Radical-radical cross-coupling 1H-TEMPO Dipp 1H p-ToISH H• abstraction -(p-ToIS)2 n-Pentane 1H₂ B. Solid-state structure of 1H-TEMPO C. Solid-state structure of 1Ha

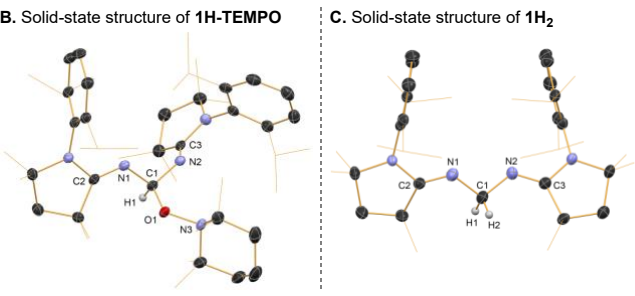


Fig. 5 | Synthesis and solid-state structure of 1H-TEMPO and 1H₂. A, Radical 1H· undergoes a radical-radical cross-coupling reaction with TEMPO to form 1H-TEMPO, and H-atom abstraction reaction with *p*-TolSH at room temperature to form 1H₂. B, Solid-state structure of 1H-TEMPO at 100 K. C, Solid-state structure of 1H₂ at 100 K. H atoms omitted for clarity, except H1 and H2. Me and ⁱPr groups are simplified as wireframes. Thermal ellipsoids set at 50% probability.

H-atom abstraction by radical 1H. One could argue that the addition of TEMPO oxygen atom to the central carbon C1 of 1H· is in part due to the high steric congestion around the ancillary carbon atoms C2/C3. To remove this ambiguity, we sought to investigate the reactivity of radical 1H· with a smaller reagent. Since H· abstraction is a classical reaction of radicals, and the small size of the H atom precludes any inherent steric biases, we subjected 1H· to p-TolSH in *n*-pentane at room temperature (Fig. 5A). This led to the immediate disappearance of the deep purple colour. NMR spectroscopy revealed the formation of methylene compound 1H₂ (as a mixture of E/E and E/Z isomers, 71% yield) resulting from H· abstraction at C1, suggesting that 1H· mimics the reactivity of a secondary carbon radical. The structure of the E/E isomer was verified by single-crystal Xray diffraction analysis (Fig. 5C). As compared with 1H, the two NHI substituents of 1H2 subtend a more acute angle of 106.8(2)° about the central carbon C1 [angle for 1H⋅: 114.5(2)°], and the central C1-N1 and C1-N2 distances [mean: 1.455(3) Å] are significantly elongated [mean distance for 1H: 1.360(2) Å]. These structural parameters are consistent with a change in hybridization of C1 from sp² to sp³ upon H• addition to 1H•.

Conclusions

More than a century after the discovery of a stable tertiary carbon radical by Gomberg, we disclose the isolation of a pentadienyl-type radical, featuring a secondary central carbon. The key to its stability is the two NHI substituents, which provide both steric protection and spin delocalization. DFT calculations confirm that the secondary carbon center is the predominant spin carrier. The H atom attached to the secondary carbon exhibits a remarkably large hyperfine coupling constant beyond 10 G, the largest recorded for an isolated organic radical. We show that **1H**• abstracts H• from *p*-TolSH to form a methylene motif, and can participate in a radical-radical cross-coupling reaction with TEMPO – the first example between two stable organic radicals.

Methods

General Consideration. All manipulations were carried out using standard Schlenk line or dry-box techniques under an atmosphere of argon. Solvents were dried over sodium benzophenone ketyl or calcium hydride, degassed and stored over activated molecular sieves or K mirror. Nuclear magnetic resonance (NMR) spectra were recorded on a Jeol 400 spectrometer, at ambient temperature unless otherwise noted. Cyclic voltammetry experiments were carried out with a CHI 600D electrochemical workstation. EPR was performed with a 9.35 GHz EMXplus-Xband CW spectrometer. Mass spectrometry was performed at the UC San Diego Mass Spectrometry Laboratory on an Agilent 6230 Accurate-Mass TOFMS spectrometer. UV-vis experiments were performed using Agilent Cary-60 UV-vis spectrophotometer. Single-crystal X-ray diffraction data were collected on Bruker Apex diffractometers using Mo-Kα radiation ($\lambda = 0.71073$ Å) or Cu-Kα radiation ($\lambda =$ 1.54178 Å) at the UC San Diego Crystallography Facility.

Starting materials

1H⁺[**TfO**⁻] was prepared according to literature procedure²⁰. All other reagents were purchased from commercial sources and used without further purification unless otherwise noted.

Preparation of 1H·. To a mixture of **1H⁺[TfO⁻]** (470 mg, 0.62 mmol) and Mg powder (47 mg, 1.93 mmol) was added THF (3 mL). The resulting suspension was subjected to ultrasonication for 4 hours, after which a deep purple solution formed. Volatiles were removed under vacuum, and solids redissolved in benzene (3 mL). The suspension was filtered off, and filtrate dried under vacuum to yield **1H·** (282 mg, 75% yield) as a dark purple solid. Single crystals suitable for X-ray diffraction were grown by slow evaporation from a concentrated solution of benzene at room temperature. **X-band EPR** g = 1.997 (1×H_{central}: 12.09 G;

2×N: 2.40 G; 2×N: 2.38 G; 1×H_{Me}: 0.70 G; 1×H_{Me}: 0.67 G). **UV-vis** (*n*-pentane, λ_{max}): 334 nm (ϵ = 7565 M⁻¹cm⁻¹), 548 nm (ϵ = 2524 M⁻¹cm⁻¹).

Author Information Corresponding authors *yloh@ucsd.edu *gbertrand@ucsd.edu

ORCID

Ying Kai Loh: 0000-0003-4019-5458 Levan Gojiashvili: 0009-0009-7504-0027 Mohand Melaimi: 0000-0003-3553-1381 Milan Gembicky: 0000-0002-3898-1612 Dominik Munz: 0000-0003-3412-651X Guy Bertrand: 0000-0003-2623-2363

Data availability: Crystallographic data for this paper (CCDC 2245614, 2267005–2267006, 2312276) are available free of charge via Cambridge Crystallographic Data Center.

Acknowledgments This work was supported by the NSF (CHE- 2246948). Thanks are due to A*STAR for a postdoctoral fellowship (YKL). The authors gratefully acknowledge the scientific support and HPC resources provided by the Erlangen National High Performance Computing Center (NHR@FAU) of the Friedrich-Alexander-Universität Erlangen-Nürnberg (FAU). The hardware is funded by the German Research Foundation (DFG). EPR work was funded by NSF MRI CHE 2019066.

Author contributions YKL conceived and performed the synthetic experiments. LG carried out the UV-vis analysis and additional synthetic experiments during revision. MM performed the EPR and electrochemical studies. MM and MG performed the X-ray crystallographic analyses. DM performed the computational work. GB supervised the project. The manuscript was written by YKL, MM and GB.

Competing interests The authors declare no competing financial interests.

Additional information
Supplementary information is available for this paper.
Experimental details (PDF).
Crystallographic data (CIF).

References

- 1. Gomberg, M. An instance of trivalent carbon: triphenylmethyl. J. Am. Chem. Soc. 22, 757–771 (1900).
- 2. Chen, Z. X., Li, Y. & Huang, F. Persistent and stable organic radicals: design, synthesis, and applications. Chem 7, 288–332 (2021).
- 3. Fessenden, R. W. & Schuler, R. H. Electron spin resonance studies of transient alkyl radicals. J. Chem. Phys. 39, 2147-2195 (1963).
- 4. Luo, Y.-R. Handbook of bond dissociation energies in organic compounds (CRC, 2002).
- 5. Stubbe, J. & Nocera, D. G. Radicals in biology: your life is in their hands. J. Am. Chem. Soc. 143, 13463-13472 (2021).
- 6. Broderick, J. B., Duffus, B. R., Duschene, K. S. & Shepard, E. M. Radical S-adenosylmethionine enzymes. *Chem. Rev.*, **114**, 4229–4317 (2014).
- 7. Bellotti, P., Koy, M., Hopkinson, M. N. & Glorius, F. Recent advances in the chemistry and applications of N-heterocyclic carbenes. *Nat. Rev. Chem.* **5**, 711–725 (2021).
- 8. Nesterov, V., Reiter, D., Bag, P., Frisch, P., Holzner, R., Porzelt, A. & Inoue, S. NHCs in main group chemistry. *Chem. Rev.* 118, 9678-9842 (2018).
- 9. Hopkinson, M. N., Richter, C., Schedler, M. & Glorius, F. An overview of N-heterocyclic carbenes. Nature 510, 485-496 (2014).
- 10. Kim, H. & Lee, E. Ambiphilic singlet carbenes: electron donors and acceptors. Bull. Korean Chem. Soc. 43, 1328-1341 (2022).
- 11. Kushvaha, S. K.; Mishra, A.; Roesky, H. W. & Mondal, K. C. Recent advances in the domain of cyclic (alkyl)(amino) carbenes. *Chem. Asian J.* 17, No. e202101301 (2022).
- 12. Melaimi, M.; Jazzar, R.; Soleilhavoup, M. & Bertrand, G. Cyclic (alkyl)(amino)carbenes (CAACs): recent developments. *Angew. Chem. Int. Ed.* **56**, 10046–10068 (2017).
- 13. Kim, Y. & Lee, E. Stable organic radicals derived from N-heterocyclic carbenes. Chem. Eur. J. 24, 19110-19121 (2018).
- 14. Kundu, S., Sinhababu, S., Chandrasekhar, V. & Roesky, H. W. Stable cyclic (alkyl)(amino)carbene (cAAC) radicals with main group substituents. *Chem. Sci.* **10**, 4727–4741 (2019).
- 15. Martin, C. D., Soleilhavoup, M. & Bertrand, G. Carbene-stabilized main group radicals and radical ions. Chem. Sci. 4, 3020-3030 (2013).
- 16. Gorodetsky, B., Ramnial, T., Branda N. R. & Clyburne, J. A. C. Electrochemical reduction of an imidazolium cation: a convenient preparation of imidazol-2-ylidenes and their observation in an ionic liquid. *Chem. Commun.* 1972–1973 (2004).
- 17. Das, A., Ahmed, J., Rajendran, N. M., Adhikari, D. & Mandal S. K. A bottleable imidazole-based radical as a single electron transfer reagent. *J. Org. Chem.* **86**, 1246–1252 (2021).
- 18. Aldeco-Perez, E., Rosenthal, A. J., Donnadieu, B., Parameswaran, P., Frenking, G. & Bertrand, G. Isolation of a C-5-Deprotonated Imidazolium, a Crystalline "Abnormal" N-Heterocyclic Carbene. *Science* **326**, 556–559 (2009).
- 19. Sau, S. C., Hota, P. K., Mandal, S. K., Soleilhavoup, M. & Bertrand, G. Stable Abnormal N-Heterocyclic Carbenes and their Applications. *Chem. Soc. Rev.* **249**, 1233–1252 (2020).
- 20. Loh, Y. K., Melaimi, M., Munz, D. & Bertrand, G. An air-stable "masked" bis(imino)carbene: a carbon-based dual ambiphile. *J. Am. Chem. Soc.* **145**, 2064–2069 (2023).
- 21. Loh, Y. K., Melaimi, M., Gembicky, M., Munz, D. & Bertrand, G. A crystalline doubly oxidized carbene. Nature 623, 66-70 (2023).
- 22. Ochiai, T., Franz, D. & Inoue, S. Applications of N-heterocyclic imines in main group chemistry. Chem. Soc. Rev. 45, 6327-344 (2016).
- 23. Goettel, J. T., Gao, H., Dotzauer, S. & Braunschweig, H. MeCAAC=N-: A cyclic (alkyl)(amino)carbene imino ligand. *Chem. Eur. J.* 26, 1136–1143 (2020).
- 24. Huynh, S., Arrowsmith, M., Meier, L., Dietz, M., Harterich, M., Michel, M., Gartner, A. & Braunschweig H. Cyclic alkyl(amino) iminates (CAAIs) as strong 2σ , 4π -electron donor ligands for the stabilisation of boranes and diboranes(4): a synthetic and computational study. *Dalton Trans.* **52**, 3869–3876 (2023).
- 25. Mahoney, J. K., Martin, D., Thomas, F., Moore, C. E., Rheingold, A. L. & Bertrand G. Air-Persistent Monomeric (Amino)(carboxy) Radicals Derived from Cyclic (Alkyl)(Amino) Carbenes. *J. Am. Chem. Soc.* 137, 7519–7525 (2015).
- 26. Styra, S., Melaimi, M., Moore, C. E., Rheingold, A. L., Augenstein, T., Breher, F. & Bertrand G. Crystalline cyclic (alkyl)(amino)carbene-tetrafluoropyridyl radical. *Chem. Eur. J.* 21, 8441–8446 (2015).
- 27. Mahoney, J. K., Jazzar, R., Royal, G., Martin, D. & Bertrand G. The advantages of cyclic over acyclic carbenes to access isolable capto-Dative C-centered radicals. *Chem. Eur. J.* **23**, 6206–6212 (2017).
- 28. Hansmann, M. M., Melaimi, M. & Bertrand, G. Crystalline monomeric allenyl/propargyl radical. *J. Am. Chem. Soc.* **139**, 15620–15623 (2017).
- 29. Regnier, V., Romero, E. A., Molton, F., Jazzar, R., Bertrand, G. & Martin, D. What are the radical intermediates in oxidative N-heterocyclic carbene organocatalysis? *J. Am. Chem. Soc.* **141**, 1109–1117 (2019).
- 30. Murphy, J. A. Discovery and development of organic super-electron-donors. J. Org. Chem. 79, 3731–3746 (2014).
- 31. Doni, E. & Murphy, J. A. Evolution of neutral organic super-electrondonors and their applications. *Chem. Commun.* **50**, 6073–6087 (2014).
- 32. Note that our calculated values are in line with those reported for the triphenylmethyl and pentadienyl radicals. See references 33 and 34.
- 33. Dalton, D. R. & Liebman, S. A. Electron spin resonance studies on neutral aromatic hydrocarbon radicals. *J. Am. Chem. Soc.* **91**, 1194-1199 (1969).
- 34. Mohos, B.; Tüdös, F. & Jókay, L. ESR investigation of the triphenylmethyl radical. *Phys. Lett. A* 24, 311-312 (1967).
- 35. Welle, F. M., Beckhaus, H.-D. & Rüchardt C. Thermochemical stability of a-Amino-a-carbonylmethyl radicals and their resonance as measured by ESR. *J. Org. Chem.* **62**, 552–558 (1997).
- 36. Griller, D., Ingold, K. U. & Walton, J. C. Two conformations of the pentadienyl radical. J. Am. Chem. Soc. 101, 758-759 (1979).
- 37. Breitwieser, K., Bahmann, H., Weiss, R. & Munz, D. Gauging radical stabilization with carbenes. *Angew. Chem. Int. Ed.* 61, e202206390 (2022).
- 38. Yi, H.; Zhang, G.; Wang, H.; Huang, Z.; Wang, J.; Singh, A. K. & Lei, A. Recent advances in radical C-H activation/radical cross-coupling. *Chem. Rev.* 117, 9016-9085 (2017).
- 39. Jeffrey, J. L.; Petronijević, F. R. & MacMillan, D. W. C. Selective radical–radical cross-couplings: Design of a formal β-Mannich reaction. *J. Am. Chem. Soc.* **137**, 8404-8407 (2015).

^{40.} Lin, Q.; Dawson, G. & Diao, T. Experimental electrochemical potentials of nickel complexes. Synlett, 32, 1606-1620 (2021).

^{41.} Azevedo, F.; Freire, C. & de Castro, B. Reductive electrochemical study of Ni(II) complexes with N₂O₂ Schiff base complexes and spectroscopic characterization of the reduced species. Reactivity towards CO. *Polyhedron* **21**, 1695-1705 (2002).